IEEE/CSC SUPERCONDUCTIVITY NEWS FORUM (global edition) October 2014.
This ASC 2014 manuscript 2MOr2B-01 published online in *IEEE Trans. Appl. Supercond.* *(IEEE XPLORE)* DOI: 10.1109/TASC.2014.2366722, on November 20, 2014.

Observation of a Bean Model Limit – A Large Decrease in Required Applied Activation Field for TFMs

Roy Weinstein, *Fellow, APS*, Drew Parks, Ravi-Persad Sawh, Kent Davey, *Fellow, IEEE*, and Keith Carpenter

***Abstract*—Experiments are reported on pulsed activation of zero-field-cooled trapped field magnets (TFMs) containing improved broken-columnar pinning centers (PCs). The YBCO TFMs have J_C ~50 kA/cm^2 and maximum trapped field, $B_{T,max}$ ~2.2 T at 77 K. Several results are in disagreement with the well-established Bean model. Essentially full activation is obtained with an applied field at the surface of $B_A \approx 1.0 \times B_{T,max}$. The Bean model predicts $B_A \geq 2 \times B_{T,max}$. Low points in activation are observed at radial sample coordinates $r \approx 0.5$ R, a result precluded by the model. Activation shows a discontinuous giant field leap, in disagreement with the smooth increase of $B_{T,max}$ vs. B_A predicted by the model. Results are compared to TFMs containing Y211 PCs, which are well described by the Bean model. E.g., for Y211 PCs, field at inner r is the last to rise. For columnar PCs it is the first to rise, an additional conflict with the model. Also, the Bean model predictions are independent of J_C, B_T, and PCs, whereas major differences exist experimentally. We speculate that with high J_C and B_T, the very large, centrally-directed Lorentz force causes a discontinuous shift of the fluxoid mesh toward $r = 0$.**

***Index Terms*—Superconducting materials, superconducting materials measurements, permanent magnets.**

I. Introduction

Much of modern infrastructure depends upon magnets. A relatively recent entry into the family of magnets is the superconducting trapped field magnet (TFM) [1]-[3]. Its advantages are that it can provide *very* high fields, stable levitation (without associated electronics) and compact, robust structure. Its disadvantages are that it must be cooled to cryogenic temperatures, and must be reactivated, if warmed.

The advantages of TFMs composed of high temperature superconductors (HTS) have encouraged a large variety of applications. For example, TFMs are used for levitating bearings in flywheels designed for energy storage. Boeing engineers report that compared to electromagnetic bearings, TFM bearings increase the time for 20% energy loss from ~10 hours to ~200 hours [4]. Other applications developed or prototyped for TFMs include motor/generator, MRI current leads, magnetic separators, water purification, magnetic field focusing, etc.

Applications of TFMs generally require that a capability for reactivation be included as an integral part of the apparatus, in the event of a warm-up. There are two basic methods of TFM activation, having different requirements and different results. These are: (1) Field-Cooled activation (FC), in which the TFM is cooled when the activating field B_A, is already present, and (2) Zero-Field-Cooled activation (ZFC), in which the activation field is applied after the TFM is cooled.

A model of the activation processes proposed in 1964 by C. P. Bean [5] has been exceptionally successful in describing and predicting the results of TFM activation. Whether for low T_C or high T_C superconductor, and whether for FC, ZFC, or pulsed-ZFC activation, this model has been repeatedly reported to successfully describe the penetration and trapping of magnetic field in Type II superconductors.

The Bean model predicts that in order for the applied field, B_A, to be large enough to fully activate the TFM via FC,

$$B_A \geq 1 \times B_{Trap,max} \quad (1)$$

where $B_{T,max}$ is the maximum trappable field of the TFM. However, for full activation via ZFC, the model requires

$$B_A \geq 2 \times B_{Trap,max} \quad (2)$$

Field-cooled activation is attractive because it requires only half the applied field of ZFC. However, in order to use the lower field permitted by FC, the field must be maintained for at least the time needed to cool the apparatus. Typically this requires more than 2 seconds.

Consider, for example, a motor capable of producing a continuous stator field of 0.5 T, with which we desire to FC activate TFMs with $B_{T,max}$ = 2.5 T. Using FC activation, 2.5 T must be applied. If activated by the stator field, this would require current increase in the stator windings by a factor of 5, an increase in heat generated by a factor of ~25, and the added current must be maintained for several seconds. In most cases, this would compromise the stator insulation. An alternative would be to place the activation wiring on the rotor. However, loss of rotor space would result in a very significant decrease in torque and torque density.

In order to avoid similar difficulties with heat and power consumption, caused by keeping activation fields on for

Automatically generated dates of receipt and acceptance will be placed here; authors do not produce these dates. This work was supported in part by the National Oilwell Varco Corporation, Houston, TX, and by the State of Texas via the Texas Center for Superconductivity at UH.

All authors are with the Texas Center for Superconductivity, and Physics Department, University of Houston, Houston, TX 77204 USA (e-mail: weinstein@uh.edu).

IEEE/CSC SUPERCONDUCTIVITY NEWS FORUM (global edition) October 2014.
This ASC 2014 manuscript 2MOr2B-01 published online in *IEEE Trans. Appl. Supercond.* *(IEEE XPLORE)* DOI: 10.1109/TASC.2014.2366722, on November 20, 2014.

seconds, most applications use ZFC activation. Although ZFC activation requires twice the field, the activating field can be applied for a very short time and provide a significantly reduced challenge to the wiring. E.g., in order to ZFC-activate a TFM capable of trapping 2.5 T, the Bean model would require an applied field of 5.0 T. The added field requires twice the current of FC activation, and four times the rate of heating. However, a pulsed field may be used for ZFC. If a pulse 30 ms long were to be used for ZFC, the stator heating would persist for a time reduced by a factor >66. The net gain using ZFC would be a factor >16 reduction in heating the activation coils.

As a result of the reduction of heating of the activation magnet coils and the energy consumed, pulsed fields for ZFC activation has been widely studied [6]-[8].

Nevertheless, as research has increased the maximum-trapped field available in a TFM from a few Gauss [9] to over 2 Tesla [10]-[11], the high field and associated current required in pulsed-ZFC activation has become a significant burden. The heating of the activating coils in a motor again tends to drive motor excitation elements onto the rotor.

In addition, having high fields enter the TFM in a short time, results in heating of the TFM itself. This acts to lower the critical current, J_C, which acts to limit the TFM to partial activation [6]. In recent literature, some groups have developed a regimen of up to 10 pulses of varying magnitude, accompanied by controlled temperature changes, to mitigate the TFM heating problem [12].

We will report in this note recent observations which permit nearly full activation using a single pulse of magnitude $B_A = 1 \times B_{T,max}$, half the value predicted by the Bean model. This substantially lower field requirement should considerably ease the difficulties inherent in remagnetizing TFM applications.

II. Prior Experiments on Low J_C, $B_{T,MAX}$ TFMs

In 2009 our group started a series of experiments on pulsed-ZFC activation to study whether any of the controllable variables could ease activation. In the first of these experiments [13], a small permanent ferromagnet was repeatedly passed through a hole in the center of a TFM, in order to study flux pumping.

The results were encouraging and the experiments were repeated with the pumping geometry approximated by a split coil, wire-wound electromagnet [14]. A schematic of the experimental apparatus is shown in Fig. 1. This geometry has been maintained for subsequent experiments, including the most recent experiment reported here. The apparatus used for the entire experimental series differs from typical pulsed activation geometries [6] in that the diameter of the activation magnet is less than the diameter of the HTS bulk sample. In most prior literature, pulsed magnets of diameter larger than the HTS were used. However, more recent reports have been made on experiments or theory using magnet diameters smaller than the HTS [13]-[16]. This geometry has been found to result in reduced heating, easier flux penetration, and more complete magnetic activation of the HTS.

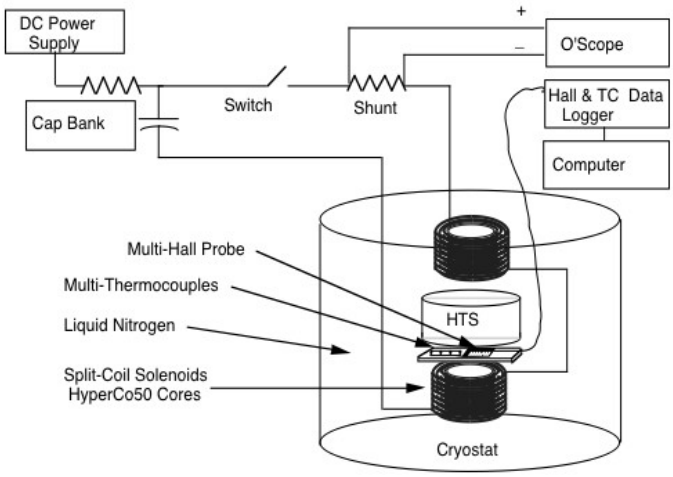

Fig. 1. Schematic of apparatus for present experiment. Earlier, lower field experiments had no thermocouples and had mild steel cores in the coils.

Each half of the split-coil electromagnet shown in Fig. 1 has 120 turns of #24 copper wire. The copper windings extend to an outer diameter of 18 mm. Until the most recent experiment the wire coils were wrapped around a core of mild steel 12 mm in diameter and 12 mm long. In the experiment reported here, Hiperco-50 cores replaced the mild steel in order to achieve higher applied fields. Activating pulses are produced by capacitive discharge. These have a rise time of ~1.2 ms, and a decay time of ~30 ms.

Hall probes and thermocouples for the experiments are placed in a gap of 1.4 mm between the bottom coil and the TFM. Seven Hall probes are placed along the 10 mm sample radius. These are positioned from $r = 1.7$ mm to $r = 8.6$ mm, and separated by 1.15 mm [17].

The TFMs used in the series of experiments are 20 mm in diameter × 8 mm long, and consist of a single grain of melt-textured YBCO.

Pinning centers (PCs) play a dominant role in determining the J_C and B_T of the TFMs. PCs are regions of non-superconducting material within the HTS, in which field can reside without violating the Meissner effect. The magnetic flux quantum resides in a lower energy state, and the PC presents an attractive potential for the flux quantum. This prevents movement of the flux, which otherwise would result in generation of dissipative electric field and loss of superconductivity.

In the earlier experiments TFMs with low J_C and B_T were studied. The PCs used in the low J_C and B_T TFMs were chemical deposits of Y_2BaCuO_5 (Y211) ranging in size from tens of nanometers to several micrometers. We will refer to the TFMs using chemical PCs as "Chem-TFMs." The Y211 deposits are made smaller, more numerous, and hence more effective, by the catalytic action of a small amount of platinum doping. The Chem-TFMs used in this experiment have characteristic $J_C \approx 15{,}000$ A/cm^2, $T_C \approx 90$ K, surface $B_{T,max} \approx 0.6$ T when not near ferromagnetic material, and $B_{T,max} \approx 0.92$ T positioned near the Hiperco-50 split magnet cores.

The early low J_C and B_T experiments were done in order to provide a base of reference of data with minimum TFM

heating. Similar experiments will be used here for comparison of high and low J_c,B_T results.

The TFMs with high B_T, J_C used in the experiment reported here, have more advanced PCs than those of Chem-TFMs. They are produced by doping the TFMs with a small amount of uranium, and irradiating with neutrons. The neutrons cause the U^{235} nucleus to split, mainly into two very energetic ions. The damage tracks left by the ions as they move through the YBCO crystal provide the non-superconducting PCs. These TFMs, like the Chem-TFMs, are 20 mm diameter × 8 mm long. We refer to TFMs produced in this way as U/n-TFMs.

In the U/n method [18]-[20] splayed (angled), columnar PCs are produced by the high-energy, high-Z ions resulting from U^{235} fission. The U/n-TFMs' pinning is greatly improved by the columnar shape of the PCs and by the fact that the diameter of the PC columns is close to the ideal diameter for pinning. The fluxoid stability is further improved because the isotropically splayed PCs cause the fluxoids of trapped field to become entangled [21], which further stabilizes the fluxoids.

Another experiment [22], done with low J_C, B_T, and the same apparatus, studied the effects of multiple pulsing. For low numbers, N, of repeated identical pulses it was found that

$$B_T(r,N) \propto k \log N, \quad (3)$$

a result suspected in an earlier experiment [13]. These characteristics were also used to cross check data in the experiments reported here.

III. TFMs and Apparatus in Present Experiment

The present experiment utilizes the same apparatus as in Fig. 1, with some changes and additions. The restricted size of the coils ($R_{MAGNET} < R_{TFM}$) makes it difficult to obtain the multi-Tesla values of B_A needed to activate TFMs of higher B_T. The mild steel cores used in the coils in the earlier experiments were replaced with cores composed of Hiperco-50. Fig. 2 shows the resulting field as a function of radial coordinate on the TFM, with coil current as a parameter.

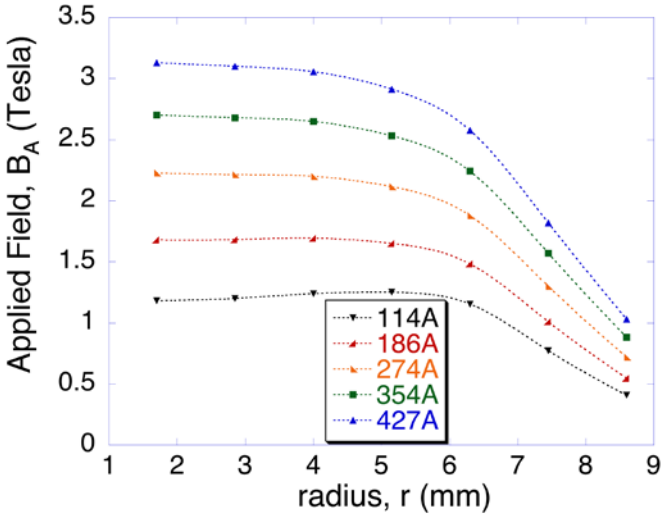

Fig. 2. Applied field B_A vs. r with coil current I_{EM} as a parameter.

In addition, since heating would be a variable of interest, four low-mass thermocouples [23] were placed opposite to the Hall probes along a radius at r = 0, 3.5, 7.5, and 9.0 mm.

IV. Experimental Results

We first consider the trapped field two minutes after the pulse. The flux flow following the 30 ms pulse lasts less than 10 seconds. By t = 2 min, B_T is governed by creep (a constant percentage loss of B_T per decade of time).

Fig. 3 shows the trapped field, $B_T(r)$ of the Chem-TFM reference sample for several values of B_A. The x-axis is the radial coordinate, r, on the TFM. The TFMs used have radius R = 10 mm hence, $0 \le r \le 10$ mm. Figs. 3 and 4 show only the instrumented region of the radius. The y-axis of the graphs is trapped field, $B_T(r)$.

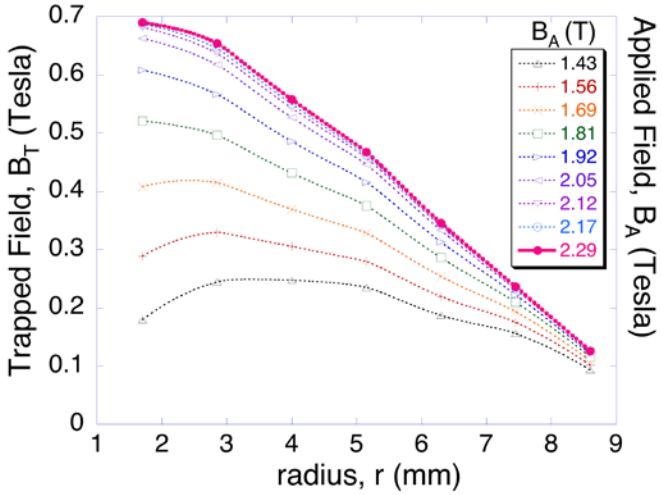

Fig. 3. Chem-TFM trapped field vs. r, with applied field as a parameter.

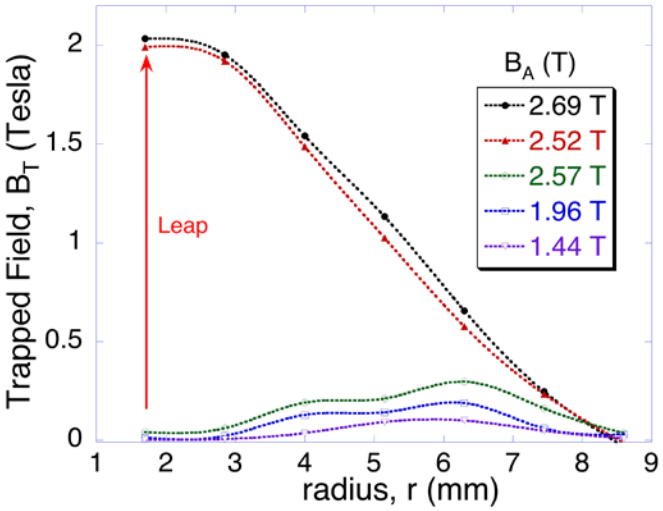

Fig. 4. U/n-TFM trapped field vs. r, with applied field as a parameter.

The behavior of the Chem-TFM is consistent with the Bean model. As B_A is increased, the maximum value of the trapped field moves from large r toward small r. In the central plane transverse to the axis of a long cylindrical TFM, the field shape predicted by the model is triangular, and the peak value of the pulsed-ZFC activated TFM is $B_{T,max}$ = ½ B_A. However, our observations are on a short cylinder at its surface, and the

field shape is modified by divergence of the field lines. The exact field shape of our finite length sample can be calculated analytically [24] or by finite element methods. $B_{T,max}$ increases smoothly as B_A increases, and the peak trapped field moves toward $r = 0$. Full activation of a Chem-TFM is obtained, as predicted by the model, at applied fields, B_A, well over twice $B_{T,max}$. Note that the excess activation field is required for it to reach further into the TFM than just the surface.

Fig. 4 shows the results for the U/n-TFM. As B_A is increased, B_T at first increases smoothly. However at one value of $B_A \equiv B_{A,leap}$ there is a sharp, very large discontinuity in $B_T(r)$. The field leaps to values close to full activation.

The Bean model permits no such sharp increase.

This giant field leap (GFL) occurs at the same value of $B_{A,leap}$ upon each of many repeated activations. Six U/n-TFMs were tested in the same manner. All exhibit the GFL at similar values of B_A. This argues against the possibility that an oddity in the grain structure of one individual TFM is responsible for the GFL.

We next compare the value of $B_T(r,B_A)$ after the leap to the value of the applied field, B_A. The maximum $B_T(r,B_A)$ occurs at $r = 0$. However, because we have no Hall probe at $r = 0$, we will compare B_T to B_A using the Hall probe closest to $r = 0$, i.e., $r = 1.7$ mm. We will compare B_T and B_A at the TFM surface, as a reasonable reference point.

The value of B_T measured by the Hall probe provides a measure of B_T at a distance of 0.7 mm from the TFM surface. The measured value of $B_{T,max}$ is ≈ 2.05 T. Finite element calculations and extrapolated experimental measurements agree that the correction of this value to the TFM surface indicates $B_{T,max}$ (r = 1.7 mm) = 2.75 T. The Bean model prediction of the minimum applied field required to achieve this activation is $B_A \geq 2 \times 2.75 = 5.50$ T. The required activation field measured at the Hall probes is $B_A \approx 2.60$ T. Finite element calculations indicate that at the sample surface, $B_A = 2.50$ T. A trapped field of 2.75 T has been attained with an applied field of 2.5 T. We estimate the errors in B_T and B_A each at ≈ ± 5%. The measured ratio of B_A to B_T is ~0.93 which, within error, is consistent with 1.0. The Bean model prediction is in disagreement with this result.

The ability to activate a TFM with greatly reduced applied field – about half the field magnitude previously thought necessary – provides for easier field generation, lower activation current, and reduced heating of both the activation coils and the TFM. It is also of importance to applications that after a dozen repeated GFLs on each of the U/n-TFMs, no TFM showed signs of deterioration.

We next ask if the U/n-TFM has been fully activated, following the GFL. The maximum trapped field for the U/n-TFM at $r = 1.7$ mm is calculated to be 3.13 T at 77 K. This value is derived indirectly because our available magnets are not capable of FC activation above 2.2 T. It was calculated from the ratio of $B_{T,max}$ of Chem-TFMs with and without Hi-50. This ratio was reduced by the effect of the saturation of the Hi-50 at the higher U/n-TFM fields. The experimental surface trapped field is $B_T(r = 1.7 \text{ mm}) \approx 2.75$ T. The 2.75 T value of B_T at $r = 1.7$ mm is 88% of full activation.

Thermocouple readings indicate a rapid temperature increase of ~3 K at $r = 3.5$ mm of the U/n-TFM, and a cool-down time of ~2 s. Slower increases of the same magnitude are seen at $r = 0$ and 7.5 mm, with comparable cooling time. No increase in temperature is seen at $r = 9.0$ mm. We have previously measured $B_{T,max}$ as a function of temperature at the National High Magnetic Field Lab in Tallahassee. We found that an increase in temperature from 77 K to 80 K resulted in a 16% decrease in $B_{T,max}$. This is in good agreement with the shortfall in B_T. We therefore attribute the shortfall to that heating. The trapped flux is ≥ 88% of maximum. The exact value depends on the geometry of the heating and the resulting non-uniform values of $J_C(r)$.

We conclude that, except for small heating effects, the GFL leaves the TFM nearly fully activated by an applied field $B_A \approx 1 \times B_{T,max}$.

The Bean model predicts that, if the superconductor is ZFC activated, then as B_A increases, the field penetration and the portions of the TFM carrying J_C start first at large r, and progresses toward small r. As this penetration occurs, the highest value of B_T progresses from large r toward $r = 0$, and increases as it progresses. This behavior is indeed observed for samples with Chem-PCs over the full range of activation [14]. However, following GFL we observe for U/n-PC samples that a low point in trapped field exists in the region $r = 4$ to 6 mm. This low point is easily seen when the GFL is caused by a value of B_A very close to the GFL threshold, $B_{A,leap}$. Fig. 5 shows such a case. As B_A is increased above the threshold for GFL, the low point increases, until it disappears. The Bean model requires $B_T(r \approx 5 \text{ mm})$ to be fully activated before B_T at lower values of r can be fully activated, and data such as shown in Fig. 5 are in conflict with the model.

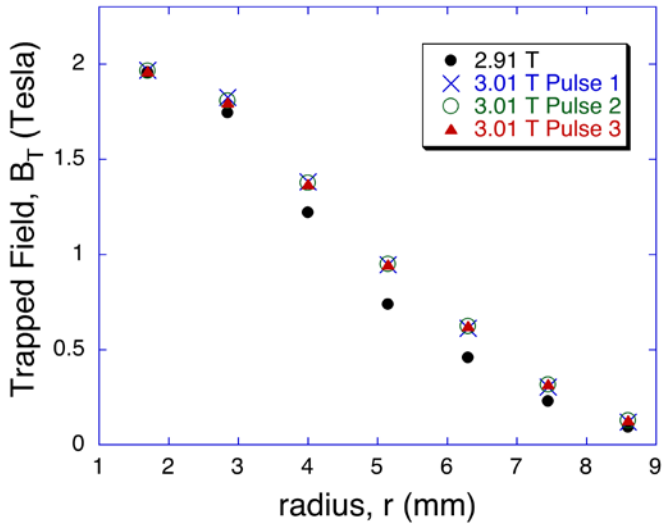

Fig. 5. Trapped field in U/n-TFM vs. r for applied field just above threshold (filled symbols) and for higher field, three sequential pulses: x, circle, and triangle.

In Figs. 6 and 7 the readout of the 7 Hall probes are shown as a function of time, with r as a parameter. Fig. 6 shows results for a sample with Chem-PCs. The field values at outer r are the first to increase. Fields at smaller r increase in

sequence after that, and the field at r = 1.17 mm is the *last* to increase. This is as described by the Bean model.

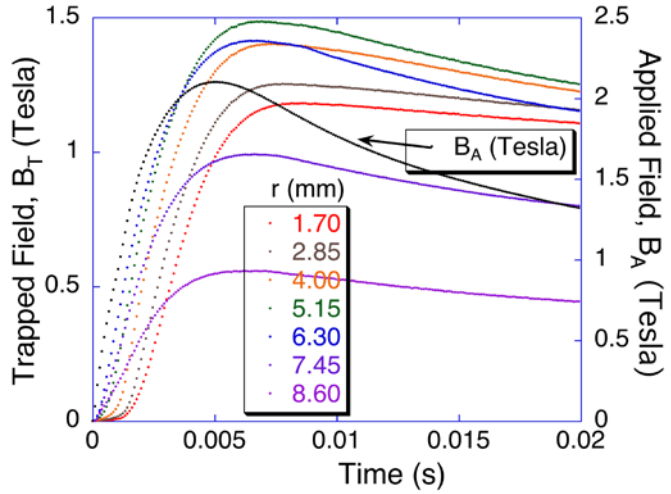

Fig. 6. Hall probe readings during applied field pulse, for Chem-TFM. Note field rises last for inner values of r.

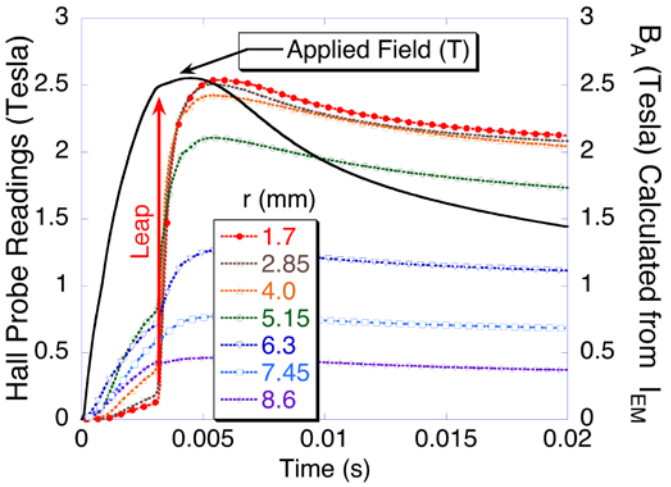

Fig. 7. As in Fig. 6, but for U/n-TFM. Note sudden rise of field for inner values of r. Note that fields at inner r rise before those at outer r.

Fig. 7 shows results for a sample with U/n-PCs. At t ~ 3 ms, following the onset of the pulse, Fig. 7 shows a rapid, very large decrease occurring in the shielding field at values of r = 1.7 and 2.85 mm, and less so at 4.0 mm. The time required for this field change is only ~1 to 2 ms. At the same time the fields at r = 5.15 mm show a smaller flux leap and in many tests show a flux decrease, depending upon the relative value of B_A and $B_{A,leap}$.

Note that the time order of activation at various r is essentially the reverse of that seen in Fig. 6, and is in disagreement with the Bean model.

Measurements of applied field, as shown in Fig. 2, were done with the YBCO bulk removed in order to distinguish B_A from the shielding effects of the YBCO. In Figs. 6 and 7 the applied field shown on the right hand y-axis is instead arrived at by measuring the current in the split-coil electromagnets, I_{EM}, and calculating field from data in Fig. 2. Since I_{EM} is measured with the TFM in place, it is affected by the field changes in the TFM. This can be used to pinpoint the time at which GFL occurs. In the repeated activations done on six U/n-TFMs, the leap always occurs within ~1 ms of the peak of B_A. This indicates that GFL can occur whether the induced electric field is opposing or aiding activation.

V. Experiments in Progress to Clarify the Conditions for GFL to Occur

It is important for applications, and interesting for basic theory, to learn more about the boundaries circumscribing the GFL. The evident variables distinguishing the U/n-TFMs in which GFL takes place from Chem-TFMs in which it does not occur, are J_C, $B_{T,max}$ and pinning centers.

Experiments in progress to distinguish the effects of each of these variables as their magnitude is varied, are: (a) an experiment to decrease the number/cm^2 of columnar PCs and observe if, and at what value, GFL goes away. This experiment will use TFMs with lower J_C, B_T, and U/n-PC density; (b) an experiment to vary the number/cc of *point* PCs, and test for GFL. This experiment will increase J_C and B_T without adding columnar PCs; (c) an experiment, like (a) but which will increase the number of columnar PCs, while decreasing J_C and B_T (via radiation damage); (d) an experiment to vary the temperature at which GFL is studied; and, (e) an experiment to vary $B_{T,max}$ while keeping J_C and PCs constant, by using thin U/n-TFMs. Results should provide a guideline for future materials development.

VI. Speculation on GFL

It has been suggested that the GFL is a consequence of heating the TFM. We find significant problems with this suggestion. The thermocouples (TCs) provide information about heating, at least as measured on a sample surface not in contact with liquid nitrogen. The TC at r = 3.5 mm shows a rapid increase in temperature of ~3 K at the time of the GFL. The TCs at 0 and 7.5 mm show a slower rise of 2-3 K. After the heating, these TCs show a cooling time of 2 s. The TFM cannot be heated to its critical temperature T_C, allow the applied field to enter, and cool to essentially recover all of its J_C, while the activating pulse is still on.

It is clear that the source of the added TFM field in the GFL may be due to penetration by the applied field. However, we speculate that it may also come from the transfer of flux within the TFM.

We speculate that the Lorentz force, F_L, plays a major role in GFL. In fully activated TFMs, F_L is directed radially outward, and is large enough to crack the YBCO ceramic during field-cooled activation [25]. However, in the case of GFL, the leap occurs at or near the point in the activation cycle at which F_L, in the region $0 < r < 5$ mm, has a maximum value directed *inward*. We speculate that the inward-directed F_L may move flux from the region r ~0.5 R, to the region near the origin.

In addition, just prior to the GFL, Fig. 5 indicates that the TFM is nearly fully activated in a direction anti-parallel to the applied field. The torque on the entangled mesh of fluxoids

can become very large, and we speculate that a flux flip, internal to the HTS, may provide flux for the GFL.

VII. Summary

At liquid nitrogen temperatures we have studied and compared pulsed-ZFC activation of TFMs with two types of pinning centers (PCs): (a) TFMs containing PCs comprised of "point" chemical deposits, and having J_C ~15 kA/cm^2 and maximum trapped field of ~0.6 T, herein called Chem-TFMs, and (b) TFMs containing splayed broken columnar PCs, and having J_C ~50 kA/cm^2, $B_{T,MAX}$ ~2.2 T, herein called U/n-TFMs.

The Chem-TFMs were studied previously and again in this work, and found to be in agreement with the Bean model. These are used here only for comparison.

The activation data for the U/n-TFMs exhibit several disagreements with the Bean model:

1. A giant field leap (GFL) occurs at a sharp, repeatable threshold of applied field, B_A, whereas the Bean model requires a smooth increase in $B_{T,max}$ as B_A is increased.
2. A U/n-TFM is essentially fully activated by a pulse magnitude $B_A \approx 1 \times B_{T,max}$, in disagreement with the Bean model result of $B_A \geq 2\ B_{T,max}$.
3. In the Bean model for ZFC activation, the outer radial regions of a TFM are fully activated before inner areas can be fully activated. Studies done during the activation pulse show that for GFL the field rise at low r occurs before that at high r. In addition, after activation, U/n-TFMs frequently exhibit a region of lower activation in the radial region r ~0.5 R. Such diminished activation is precluded by the model.
4. The Bean model predicts the same behavior pattern for high J_C and B_T as for low J_C and B_T. The model's predictions are also independent of the *method* of obtaining high J_C and $B_{T,max}$, such as by improved pinning centers. In particular it allows for no difference between behavior of HTS containing columnar PCs and that of HTS containing point PCs. However, significant differences are observed.

Six U/n-TFMs, with the same production protocols, all exhibited GFL with thresholds at comparable values of B_A, indicating that the GFL is not due to a crystal peculiarity of an individual TFM.

Surface temperature measurements, at a surface not directly exposed to the coolant, indicate a rapid temperature rise of 3 K accompanying GFL, and a cooling time of ~2 seconds. We believe that the magnitude and duration of the temperature changes precludes GFL being caused by a thermal fluctuation.

The results are encouraging for TFM applications. The observed maximum trapped field following the GFL is equal to the pulse magnitude within the experimental error of ~7%. The observed maximum trapped field is below the theoretically achievable maximum by ~12%. This shortfall is in good agreement with the decrease in J_C expected to accompany a 3 K increase in temperature. Repeated GFLs do not deteriorate the TFM. These characteristics make the GFL a very valuable assist for applications.

Acknowledgment

We thank Prof. Chin-Sen Ting of the UH Physics Dept. for discussions concerning the anomalous Hall effect, and Prof. Archie Campbell of the University of Cambridge for suggestions of possible causes of the GFL.

References

[1] M. Rabinowitz, U.S. Patent # 4,176,291.
[2] M. Rabinowitz, H. W. Arrowsmith, and S. D. Dahlgren, "Dependence of maximum trappable field on superconducting Nb_3Sn cylinder wall thickness," *Appl. Phys. Lett*., vol. 30, pp. 607-609, 1977.
[3] R. Weinstein, U.S Patent # 7,667,562.
[4] George Roe, "Boeing Flywheel Energy Storage," Boeing Research and Technology Report, 2012.
[5] C. P. Bean, "Magnetization of high-field superconductors," *Rev. Mod. Phys*. ,vol. 36, pp. 31-39, 1964.
[6] G. Krabbes, G. Fuchs, W.-R. Canders, H. May, R. Palka, "High Temperature Superconductor Bulk Materials," Wiley-VCH Verlag GmbH and Co. KGaA, Weinheim, Germany, 2006.
[7] B. P. Martins, Ed., "New Topics in Superconductivity Research," Nova Science Publishers, 2006.
[8] Y Kimura, et al., "Recovery of trapped field distribution around a growth sector in a Gd-Ba-CU-O HTS bulk with pulsed-field magnetization," *Supercond. Sci. Technol.*, vol. 19, no. 7, pp. S466-S471, 2006.
[9] R. Weinstein, I.G. Chen, J. Liu, D. Parks, V. Selvamanickam, and K. Salama, "Persistent magnetic fields trapped in high T_c superconductor," *Appl. Phys. Lett.* vol. 56, 1475-1477, 1990.
[10] R. Weinstein, R. Sawh, Y. Ren, D. Parks, "The role of uranium, with and without irradiation in the achievement of $J_c \approx 300{,}000$ A/cm^2 at 77K in large grain melt-textured Y123," *Mater. Sci. Eng*. B vol. 53, pp. 38-44, 1998.
[11] R.-P. Sawh, R. Weinstein, K. Carpenter, D. Parks, K. Davey, "Production run of 2 cm diameter YBCO trapped field magnets with surface field of 2 Tesla at 77 K." *Supercond. Sci. Technol.* vol. 26, no. 10, Oct. 2013, Art. No. 105014.
[12] D. Zhou, et al., "An overview of rotating machine systems with high temperature bulk superconductors," *Supercond. Sci. Technol*. vol. 25, no. 10, Aug. 2012, Art. No. 103001.
[13] R. Weinstein, D. Parks, R.-P. Sawh, and K. Davey, "Measurements of flux pumping activation of trapped field magnets," *Supercond. Sci. Technol.*, vol. 23, no. 11, Oct. 2010, Art. No. 115015.
[14] R. Weinstein, D. Parks, R.-P. Sawh, and K. Davey, "Characteristics of trapped field magnet activation by flux pumping." *IEEE Trans. Appl. Supercond.*, vol. 21, no. 3, Part II, pp. 2436-2440, 2011.
[15] Z. Xu, R. Lewin, A. M. Campbell, D. A. Cardwell, H. Jones, "Simulation studies on the magnetization of (RE)BCO bulk superconductors using various split-coil arrangements," *Supercond. Sci. Technol*. vol. 25, no. 2, Jan. 2012, Art. No. 025016.
[16] Z. Deng, et al., "The effectiveness of pulsed magnetization with respect to different performance superconductors," *J. Supercond. Nov. Magn.*, vol. 25, pp. 61-66, 2012.
[17] Arepoc, S.R.O., Bratislava Slovakia. #M7-TH7B Multi-Hall probes. Available: www.arepoc.sk.
[18] R. Weinstein, U.S. Patents # 6,083,885 and # 6,525,002.
[19] R. Weinstein, R.-P. Sawh, D. Parks, B. Mayes, "Improvement of high T_c superconductor by near-optimum pinning centers created by high Z, high-energy ions." *Nuclear Instruments and Methods in Physics Research B,* vol. 272, pp. 284-290, 2012.
[20] R. Weinstein, et al., "Properties of HTS for successful U/n processing," *Physica* C vol. 341-348, pp. 1415-1418, 2000.
[21] D. R. Nelson, "Vortex entanglement in high-Tc superconductors," *Phys. Rev. Lett.* vol. 60, pp. 1973-1976, 1988.
[22] R. Weinstein, D. Parks, R.-P. Sawh, K. Davey, and K. Carpenter, "A study of pulsed activation of trapped field magnets: effects of multiple pulsing," *Supercond. Sci. Technol.* vol. 26, no. 9, July 2013, Art. No. 095005.
[23] Omega Engineering; # CO2-T, Thickness 0.0005", 2 ms response thermocouples.

[24] Jay Liu, Ph.D. dissertation, Physics Dept., University of Houston, Houston, TX, USA, 1994.
[25] Y. Ren, R. Weinstein, J. Liu, and R. P. Sawh, C. Foster, "Damage caused by magnetic pressure at high trapped field in quasi-permanent magnets composed of melt-textured YBaCuO superconductor," *Physica* C vol. 251 pp. 15-26, Sept. 1995.